

PRODUCTION OF 25 MeV PROTONS IN CO₂ LASER-PLASMA INTERACTIONS IN A GAS JET*

D. Haberberger, S. Tochitsky, C. Gong, C. Joshi

Neptune Laboratory, Department of Electrical Engineering, UCLA, Los Angeles, CA, USA

Abstract

At the Neptune Laboratory at UCLA, we have developed a high-power CO₂ MOPA laser system which produces world record, multi-terawatt 10 μ m pulses. The CO₂ laser pulses consist of a train of 3ps pulses separated by 18ps, each with a peak power of up to 4TW and a total pulse train energy of \sim 100J. These relativistic laser pulses are used for Laser Driven Ion Acceleration in a H₂ gas jet operated around the critical density of 10¹⁹cm⁻³ for 10 μ m. The laser is focused into the gas jet reaching a normalized field strength of a₀ \sim 2 in vacuum. For these conditions, protons with a maximum energy of 25MeV and a narrow energy spread of $\Delta E/E \sim 1\%$ are recorded. Initial analysis of these experimental results shows a stronger scaling of the proton energy than that predicted from the ponderomotive force, and highlights the importance of an accumulated effect of multiple CO₂ laser pulses lasting over 100ps. The temporal dynamics of the overdense plasma slab are probed with a picosecond 532nm pulse and the results will be discussed.

INTRODUCTION

Laser-driven ion acceleration (LDIA) has attracted interest from the scientific community due to the compact nature of the accelerator and unique qualities of the accelerated ion beams such as ultra-low emittance and short duration. LDIA produced ion beams have been proposed for use in fast ignition in inertial confinement fusion, as a diagnostic tool for probing the electric fields in high temperature plasmas, and for proton beam cancer therapy [1].

Here we present experimental results on LDIA in a H₂ gas jet when a multi-terawatt 10 μ m time-structured laser pulse is used for proton acceleration. Gas jets have the advantage of precise plasma density control in the range of 10¹⁸-10²⁰cm⁻³ around the critical density of 10 μ m (n_{cr}=10¹⁹cm⁻³). Also they provide a debris free plasma source at a high repetition rate (1-10Hz) which is difficult to accomplish with solid density targets.

LDIA EXPERIMENTAL SETUP

The drive laser used for the LDIA experiment is a CO₂ master oscillator-power amplifier system, built at the UCLA Neptune Laboratory, capable of producing multi-terawatt picosecond pulses containing \sim 100J. A detailed description of this laser system can be found elsewhere [2]. Due to a modulated gain spectrum of the CO₂ molecule, the amplification of a picosecond pulse results in a pulse

train with a pulse separation of 18ps and an individual pulsewidth of $\Delta\tau \sim 3$ ps. A typical output of the final amplifier as measured by a streak camera is seen in Fig. 1 where one can see the peak powers of \sim 4TW is achieved.

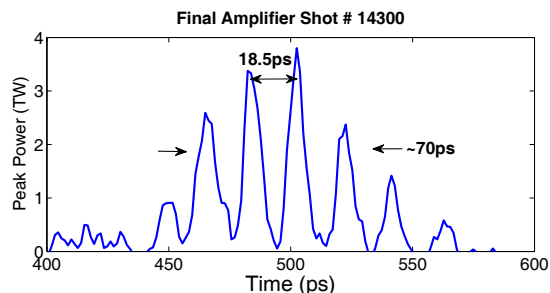


Figure 1: Temporal profile of a 10 μ m pulse train after final amplification in the CO₂ 3-pass amplifier as measured by a streak camera.

Approximately 50J of the CO₂ laser beam is coupled into the vacuum target chamber (shown in Fig. 2) where it is focused by an F/1.5 off-axis parabolic (OAP) mirror onto a H₂ gas jet. For each shot, a temporally resolved 3ps pulse train is recorded using a streak camera diagnostic and the light reflected back from the plasma is measured.

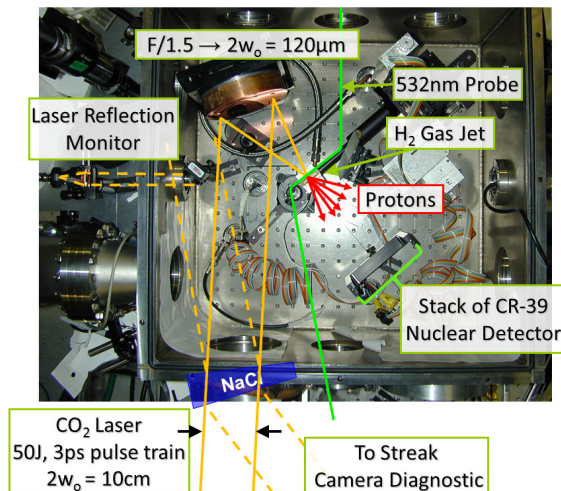


Figure 2: Picture of the LDIA target chamber.

The H₂ gas jet is characterized at a height of 1mm above the nozzle using plasma density interferometry. These measurements reveal a quasi-triangular neutral gas density profile with a FWHM of \sim 800 μ m. The peak density can be varied from 5x10¹⁸ to 10²⁰cm⁻³ which corresponds to 0.5 to 10 times the critical plasma density for 10 μ m light.

*Work supported by DOE grant DE-FG02-92-ER40727

Protons accelerated in the forward direction are detected with a stack of CR-39 nuclear track detectors, which are not sensitive to electrons and X-rays produced in the plasma. By analyzing the penetration depth of protons, using a calculated Bragg peak value for each energy, it is possible to recover the energy spectrum of the accelerated protons. Our CR-39 detector covers an area of $100 \times 100 \text{ mm}^2$ acting as a 2D imaging spectrometer and is placed 150mm behind the gas jet subtending an half-angle of 18° .

LDIA EXPERIMENTAL RESULTS

$10\mu\text{m}$ Laser Focus Measurements

The focal volume of the $10\mu\text{m}$ laser beam is characterized using an IR camera with a magnifying imaging system. The spatial profile of the beam was measured (without final amplification) while scanning along the laser axis (denoted \hat{z}). Due to residual astigmatism of the beam, a horizontal (w_h) and vertical (w_v) radius is extracted for each \hat{z} position and plotted as seen in the blue and green traces in Fig. 3. The red trace is an effective radius calculated as $w_{eff}^2 = w_h \cdot w_v$, which represents the intensity distribution of the laser beam. The dashed lines represent ideal Gaussian beam profiles for an F/1.5 (black) and an F/3 (brown) focusing geometry.

The measured spot size for the unamplified beam is $w_o = 70\mu\text{m}$. However, due to a smaller beam diameter for the unamplified beam, it follows an F/3 focusing geometry. After final amplification, a 10cm beam is sent onto the OAP; therefore, the F/1.5 focusing geometry should result in a smaller spot size. For a non-Gaussian (large M^2) beam, we estimate the focused spot size to be $w_o \sim 60\mu\text{m}$. For a typical pulse train as shown in Fig. 1, this corresponds to peak intensities up to $3.3 \times 10^{16} \text{ W/cm}^2$, or a normalized vector potential of $a_o \sim 1.8$ for $10\mu\text{m}$ radiation.

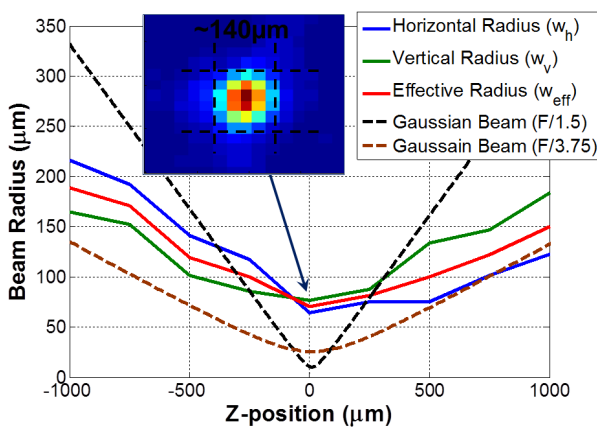


Figure 3: $10\mu\text{m}$ laser beam radius compared to ideal Gaussian beam radius plotted along the laser axis (\hat{z}).

Picosecond Plasma Diagnostics

The plasma density profile is probed with a 3ps 532nm (Nd:Glass frequency doubled) pulse synchronized with the high power $10\mu\text{m}$ pulse train. The experimental setup of the probe pulse is depicted in Fig. 4.

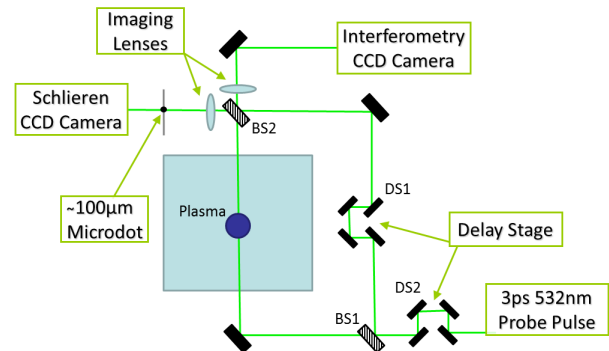


Figure 4: Schematic of the 3ps 532nm probe pulse setup for interferometry and schlieren plasma profile measurements.

The probe beam is split and combined at the beam splitters (BS1 and BS2) in a standard Mach-Zehnder interferometry setup. A delay stage (DS2) is placed in the reference arm to temporally overlap the two pulses at BS2. An imaging lens then transfers the image plane of the plasma to the interferometry CCD camera with a measured resolution of $\sim 20\mu\text{m}$.

In addition to interferometry, the part of the plasma arm that reflects off of BS2 is used to create a schlieren image of the plasma. A dark field schlieren technique is used for analysis of the plasma density gradients [3]. A $\sim 100\mu\text{m}$ dot printed on a transparency and aligned to the focus of the probe beam is used as a beam block. The measured resolution of the schlieren images is $\sim 35\mu\text{m}$.

Due to the fact that the $10\mu\text{m}$ seed pulse and the 532nm probe pulse both originate from the same $1\mu\text{m}$ pulse [2], they are inherently synchronized. However, due to different lengths in transport, the two pulses must be temporally overlapped at the interaction point (IP) with picosecond accuracy. For this purpose, we used a Si semiconductor switch for a cross-correlation measurement. Here, a piece of Si is placed at the IP which normally transmits a large fraction of the $10\mu\text{m}$ light but absorbs the 532nm light with a photon energy exceeding the bandgap of Si. As the 532nm photons are absorbed, an electron-hole plasma is formed on the surface of the Si eventually modulating the transmission/reflection of the $10\mu\text{m}$ light as the plasma density reaches n_{cr} for $10\mu\text{m}$ light.

The results of the cross-correlation measurement are shown in Fig. 5a. The data points represent the normalized transmission of $10\mu\text{m}$ light through the Si versus the delay in the probe pulse. When the probe pulse arrives early, the $10\mu\text{m}$ light is screened by the plasma, and when the probe arrives later the $10\mu\text{m}$ light is transmitted. The blue dashed line represents a fit to the data and the solid green

line is the derivative of the fit. This derivative then correlates to the temporal width of the $10\mu\text{m}$ pulse train which was measured to be $\sim 160\text{ps}$ (FWHM). Fig. 5b shows a typical streak camera image where the temporal delay between the $10\mu\text{m}$ pulse train and the 532nm probe represents probing in the middle of the pulse train. Thus by recording timing of the amplified CO_2 laser pulse train and the 532nm probe, one can define the probing time to within $\pm 20\text{ps}$.

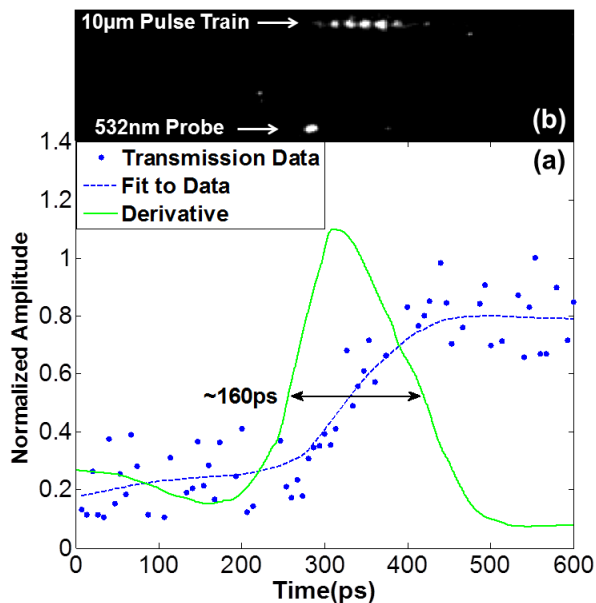


Figure 5: Cross-correlation of the 3ps 532nm probe pulse with the $10\mu\text{m}$ pulse train.

A typical result of plasma interferometry is shown in Fig. 6a. The probe timing is $\sim 70\text{ps}$ after the peak of the pulse train and the peak neutral gas density is $3.5 \times 10^{19}\text{cm}^{-3}$. Due to strong turbulence in plasmas driven by the 50J $10\mu\text{m}$ pulse trains, direct computational analysis of the interferogram is very difficult. Therefore a simulated interferogram (Fig. 6b) generated from a 3D model plasma is used as a guidance. The 3D shape used for the plasma is a paraboloid with a cross-sectional profile shown in Fig. 6c (lineout denoted by the blue dashed line in Fig. 6b).

Two main conclusions can be drawn from the comparison between the experimental and simulated interferograms. First, the laser has modified the plasma density profile through radiation pressure forming a sharp rise on the front side of the profile where the laser is stopped by the critical density layer. Although refraction caused by strong plasma density gradients behind the critical layer has resulted in the loss of some probe light, the first two fringes are visible (traced by dashed blue lines). Second, a column of low density plasma formed on the back side shows an exponential decrease in plasma density from the critical layer to our resolution limit (10^{18}cm^{-3}) in a $\sim 400\mu\text{m}$.

These ultrathin plasma density profiles, dynamically evolved from the much wider neutral gas jet, having a sharp

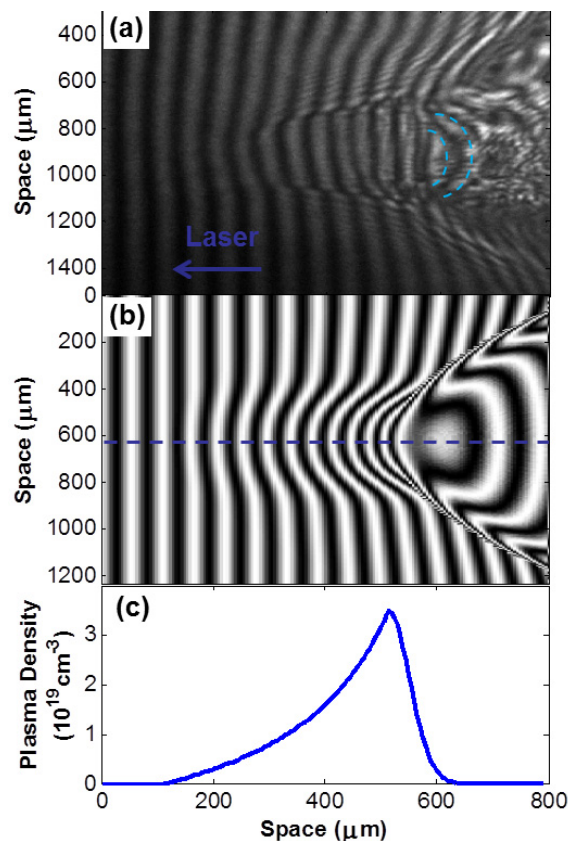


Figure 6: Interferogram obtained at a peak plasma density of $3.5 \times 10^{19}\text{cm}^{-3}$ (a), simulated interferogram (b), and its corresponding longitudinal plasma profile (c).

rise ($< 10\lambda$) and exponential fall ($\sim 40\lambda$) facilitate efficient shock launching by multiple 3ps pulses. In the experiment we detected forward accelerated proton beams with a narrow energy spread. The maximum energy fluctuates from shot to shot in the range of $15\text{--}25\text{MeV}$. The measured energy spread is $\Delta E/E \sim 1\%$

CONCLUSION

We have presented the results of a Laser Driven Ion Acceleration experiment involving the interaction of a high-power time-structured $10\mu\text{m}$ pulse train with a near critical density H_2 gas jet. This interaction forms a unique ultrathin, overdense plasma density profile which allows for the production of protons with a narrow energy spread. Existence of this plasma density profile is shown through time resolved interferometry and schlieren images produced by a 3ps 532nm probe pulse.

REFERENCES

- [1] K.W.D. Ledingham and W. Galster, *New J. Phys.* 12, 045005 (2010).
- [2] D. Haberberger et al., *Opt. Exp.* 18 (2010) 17865.
- [3] G.S. Settles, *Schlieren and Shadowgraph Techniques* (Springer-Verlag, Berlin, 2001).